MINORITY CARRIER LIFETIME IN CRYSTALLINE AND POLYCRYSTALLINE SILICON SOLAR CELLS

A Thesis Presented to the

the School of Graduate Studies

Addis Ababa University

In Partial Fulfillment

of the Requirement for the Degree

of Master of Science In Physics

BY

ELIAS LEWETEGN

ADDIS ABABA

JUNE 1999

ACKNOWLEDGEMENT

I am indebted to Dr. Ulrich Stutenbaeumer for his consistent guidance and encouragement. Moreover, I thank him for providing his own private materials for this work without reservation.

I would like to thank the Physics department of the AAU for providing the necessary materials for this work. I wish to express my gratitude to Dr. Fesseha Kassahun for facilitating my work and Dr. Araya Asfaw for technical support and encouragement throughout my work.

Furthermore, I would like to extend my warmest gratitude to my wife, Alem Assefa, and all frinds of mine for their material and moral support. The effort of my children namely: Bruktait, Mikias, Brehan, Hewan and Meron was also worth mentioning in facilitating my activities while conducting my study at home.

Last but not least, I wish to thank to Hetosa Wereda Educational Bureau, Arsi Administrative zone, for granting me the sponsorship to join the school of graduate studies in AAU.

ABSTRACT

The photoinduced open-circuit voltage decay technique was used to investigate the minority carrier lifetime in crystalline and polycrystalline silicon solar cells. This convenient investigation technique allows a fast determination of the minority carrier lifetime in semiconductor materials and is an important technique to predict the solar cell performance. The decay curves were obtained with a xenon stroboscope lamp and Nd:YAG laser and Nitrogen laser pulses as an excitation source.

CONTENTS

LIST OF FIGURES

1. INTRODUCTION

The conversion of sunlight directly into electricity using solar cells can provide a limitless energy source. Consequently the demand for photo-voltaic systems has increased through out the world. In developing countries such as Ethiopia, where the settlement are scattered, the electric infrastructure is limited and the sunlight is plentiful, the need for solar energy resources is essential.

Photo-voltaic (PV) systems are currently the most effective developed method for directly generating electricity from light and scientists and engineers are working to increase the efficiency of PV systems and to reduce the cost.

Crystalline silicon (Si) cells are the most frequently used system parts in PV energy conversion.

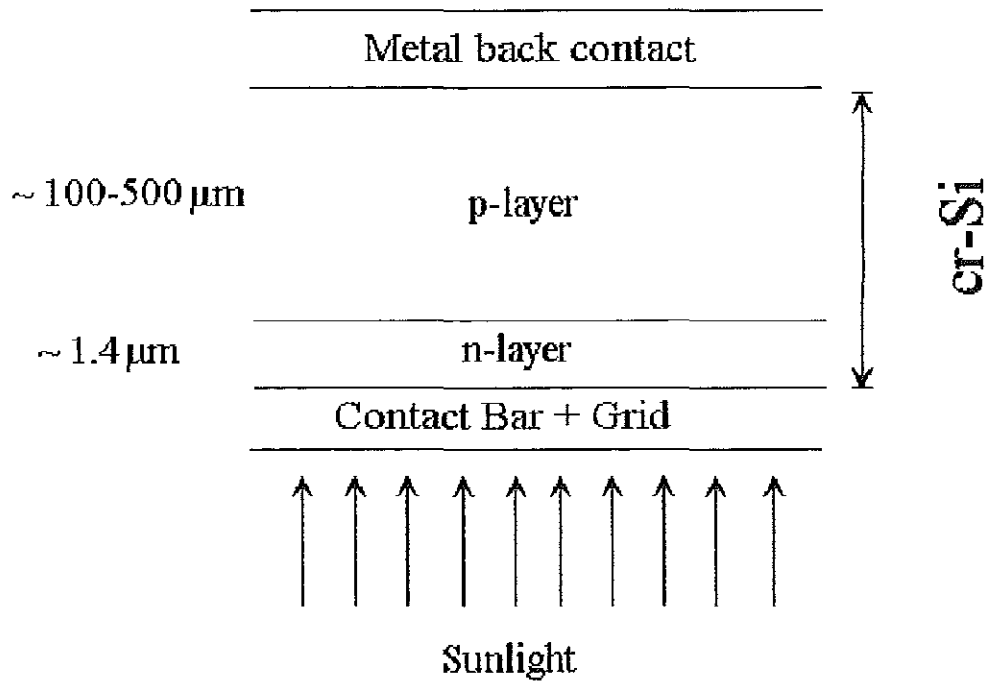

Figure 1.1 *Schematic diagram of a crystalline silicon solar cell[7].*

Thus, the interest in crystalline Si has continued to grow [7]. A crystalline Si pn junction solar cell consists of a relatively small n-type emitter and a much thicker p-type base (Fig.1.1).

The minority carrier diffusion length (MCDL) has been widely used to characterize

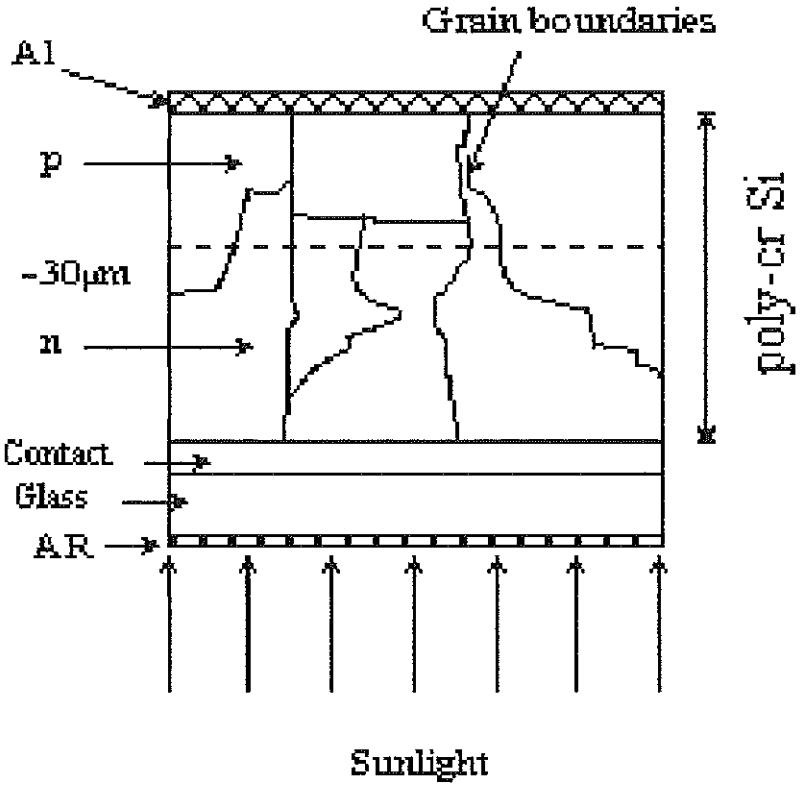

***Figure 1.2** Schematic diagram of a thin film polycrystalline silicon solar cell . AR abbreviates anti-reflection coating [1].*

the quality of Si solar cell materials before processing, because it provides a prediction of the energy conversion efficiency that may be attained in the final cell [8].

In addition, precise determination of this parameter is crucial for accurate simulations of the transport characteristics of semiconductor devices such as high efficiency Si solar cells.

The photo-induced open-circuit voltage decay technique was originally introduced by Gossick [9]. It involved creating excess minority carriers in a junction device using an external excitation provided by a brief forward current, and monitoring the open-circuit voltage, V_{oc}, after the excitation has been abruptly terminated. Minority carrier lifetime can be determined by analyzing the resultant V_{oc} decay curve.

Further lifetime studies are required to determine the possibilities and limitations of new solar cell designs with high efficiencies [8].

Various methods have been reported for the determination of the lifetime of minority carriers or their diffusion length. The photo-conductive decay (PCD) method has been used for the measurement of the minority carrier lifetime by a number of investigators. The surface photo-voltage (SPV) technique is also a convenient method of measuring the minority carrier diffusion length L which is related to the diffusion coefficient D and the minority carrier lifetime τ. In the PCD method, the crystal is illuminated by a pulse of light and the relation of the PCD pulse amplitude with the applied electric field is studied graphically. The SPV method for measuring the minority carrier lifetime utilizes a beam of photons incident on the surface of the semiconductor at an energy just above the band gap. These methods are based on optical and electrical techniques. For solar cells, it is appropriate to determine the lifetime using an optical method [8].

In this investigation the minority carrier lifetimes of crystalline and polycrystalline Si solar cells are determined using photo-induced open-circuit voltage decay (OCVD)

with Nd:YAG and Nitrogen lasers as an excitation sources and are compared with those obtained with a stroboscope lamp as an excitation source. The applied photo-induced OCVD technique is simple and straightforward, requires no complicated technique and expensive equipment but nevertheless achieves reliable experimental results [9,15].

This thesis is divided into six sections. Section 2 describes the theory relating the minority carrier lifetime to other semiconductor parameters. The open-circuit voltage decay, the decay time and the minority carrier diffusion length are discussed starting from the basic continuity equation. The characteristics of solar cells are a function of optical energy, which is absorbed in a semiconductor and generates excess electron-hole pairs producing photocurrents. The output terminals of the solar cell are connected to a resistive load so that input optical power is converted to electrical power. The knowledge of various characteristics including the short-circuit current, the open-circuit voltage, optical absorption, maximum power and conversion efficiency of a Si solar cell is of basic importance in designing the devices [4]. The optical and electrical properties of Si solar cells are also discussed in section 2. Section 3 contains a description of the experimental apparatus and the procedures to carry out OCVD measurements. In the fourth section the results of this investigation are presented and the discussion of the data and graphs are given. In section 5 concluding remarks are given and finally the reference materials are listed in section 6.

2. THEORY

2.1 Minority carrier lifetime in semiconductors

The basic equations for semiconductor device operation are those which describe the static and dynamic behaviour of carriers in semiconductors under the influence of external fields which cause deviation from the thermal equilibrium conditions.

In the discussion the following representations are used.

n_{po} - thermal equilibrium concentration of minority carrier electrons

p_{no} - thermal equilibrium concentration of minority carrier holes

J_p - minority carrier hole diffusion current density

J_n - minority carrier electron diffusion current density

D_p - hole diffusion coefficient

D_n - electron diffusion coefficient

L_p - diffusion length in the p side

L_n - diffusion length in the n side

n_p , p_n - minority carrier densities

E – Applied electric field

Let us consider the case when a semiconductor sample is illuminated with light and the electron hole pairs are generated uniformly throughout the sample with a generation rate G . The boundary condition are $E = 0$ and $\frac{\partial p_n}{\partial x} = 0$ Starting from the continuity equation we have the equation in the form [4,12] :

$$\frac{\partial n_p}{\partial t} = G - \frac{n_p - n_{po}}{\tau_n} \qquad (2.1)$$

At steady state, $\frac{\partial n_p}{\partial t} = 0$ and $n_p = n_{po} + \tau_n G$

Where τ_n is the minority carrier lifetime in p-type semiconductor.

If the light is turned off at t=0, the boundary conditions are $n_p(0) = n_{po} + \tau_n G$ and $n_p(t \to \infty) = n_{po}$ then the solution is:

$$n_p(t) = n_{po} + \tau_n G \qquad (-t/\tau_n) \qquad (2.2)$$

This expression presents the main idea of the Stevenson-Keys method for measuring the minority carrier lifetime.

Also the net movement of charge due to an electric field gives rise to a drift current. Since electrons and holes contribute to the drift current, the drift current density is given by [4]:

$$J_{drf} = e(\mu_n n + \mu_p p)E \qquad (2.3)$$

Where J_{drf} is the drift current density, μ_n is the electron mobility, μ_p is the hole mobility and E is the electric field.

The drift current density can also be written as:

$$J_{drf} = e(\mu_n n + \mu_p p)E = \sigma E \qquad (2.4)$$

Where σ is the conductivity of the semiconductor material. Then the conductivity becomes:

$$\sigma = e(\mu_n n + \mu_p p) \qquad (2.5)$$

The excess carriers generated uniformly throughout the sample by the light pulses cause a momentary increase in the conductivity. The increase manifests itself by a drop in the voltage across the sample when a constant current is passed through it. This decay can be observed on an oscilloscope screen and is a measure of the lifetime. But the pulse width must be much less than the life time.

Using the photo-induced OCVD technique, excess minority carriers are created in a junction device using an external pulsed optical excitation that creates a brief forward current [9].

The variation of V_{oc} with time for a device in the decay mode is a graph which has three distinct regions. The first region corresponds to a condition of high-level injection, where the excess minority carrier concentration exceeds the majority carrier concentration in the base region of the cell. When this condition is met, the decay curve is linear and the minority carrier life time (τ) may be described using the following expression [9]:

$$\tau = 2\frac{kT}{q}\left|\frac{1}{dV_{oc}/dt}\right| \qquad (2.6)$$

where k is Boltzmann`s constant, T is the absolute temperature, q is the elementary charge, and t is the time.

The second region of the decay curve corresponds to a condition of intermediate injection, where the excess minority carrier concentration in the base is greater than the thermal-equilibrium minority carrier concentration but less than the thermal-equilibrium majority carrier concentration. Under these conditions the decay curve is again linear, and the lifetime can be computed from the following expression [9] :

$$\tau = \frac{kT}{q}\left|\frac{1}{dV_{oc}/dt}\right| \qquad (2.7)$$

Finally, in the third region of the decay curve, low-injection condition exists, where the excess minority carrier concentration is less than the equilibrium minority carrier concentration. As V_{oc} becomes much less than kT/q, the V_{oc} decay approaches the following time dependence:

$$V_{oc} = \frac{kT}{q}\left[\quad \left(\frac{qV_o}{kT}\right) - 1\right] \quad \left(\frac{-t}{\tau}\right) \qquad (2.8)$$

where V_o is the open circuit voltage at the termination of excitation. An exponentially decaying low injection curve is mostly determined by the RC time constant of the solar cell.

Diffusion length, L, is defined as the mean distance a minority carrier travels before recombination.

At a distance x into the base [7]:

$$\Delta n(x) = \Delta n(0) \quad \left(\frac{-x}{L}\right) \qquad (2.9)$$

The probability that an electron injected at x=0 survives to a distance x is :

$$\frac{\Delta n(x)}{\Delta n(0)} = \qquad \left(\frac{-x}{L}\right) \qquad (2.10)$$

The probability that an electron at x will recombine at x+dx is:

$$\frac{\Delta n(x)-\Delta n(x+dx)}{\Delta n(x)} = \left(\frac{-d\Delta n(x)}{dx}\right)\left(\frac{dx}{\Delta n(x)}\right) = \frac{dx}{L} \qquad (2.11)$$

By taking the product of the above two probabilities, the probability that an electron injected at x=0 will recombine at a given dx is :

$$\left(\frac{-x}{L}\right).\left(\frac{dx}{L}\right)$$

Then the medium distance that an electron diffuses before recombining is :

$$\langle x\rangle = \int_o^\infty x \qquad \left(\frac{-x}{L}\right).\left(\frac{dx}{L}\right) = L \qquad (2.12)$$

Thus diffusion length is both the medium distance before recombination and the exponential decay length.

Substituting the expression for minority carrier lifetime τ in the Einstein equation for the diffusion length [4] :

$$L = \sqrt{D\tau} \qquad (2.13)$$

with the diffusion constant

$$D = \left(\frac{kT}{q}\right)\mu_h \qquad (2.14)$$

where μ_h is the mobility of holes in the respective material of the solar cell, the diffusion length can be calculated from :

$$L = \sqrt{\left(\frac{kT}{q}\right)\mu_h \tau} \qquad (2.15)$$

Careful measurements of the V_{oc} decay and dt of the second part of the curves obtained from the crystalline and polycrystalline silicone solar cells will be used to determine the minority carrier lifetimes from equation (2 . 7). So the minority carrier diffusion length can be determined by the OCVD method.

2.2. *Optical and electrical properties of solar cells*

2.2.1 Optical properties of solar cells

Optical measurements are frequently used to determine the band structures of semiconductors. Photon-induced electronic transitions can occur between different bands which lead to the determination of the energy gap; or within a single band such as the free-carrier absorption. Optical measurements can also be used to study lattice vibrations. When a beam of light is incident on a semiconductor material, the light reflected or transmitted by the material can be described by optical parameters such as refractive index n, absorption coefficient α, extinction coefficient k, and optical energy gap E_g^{opt} [12].

Light incident on a semiconductor is attenuated as it passes through the semiconductor. The rate of light absorption is proportional to the photon flux at a given wavelength. The intensity of monochromatic light as it passes through the semiconductor is described mathematically as

$$I(x) = I_o \qquad (-\alpha x) \qquad (2.16)$$

where α is the absorption coefficient. The absorption coefficient determines how far below the surface of the solar cell light of a given wavelength is absorbed. Photon interaction with a valence electron creates an electron in the conduction band and a hole in the valence band-an electron-hole pair. Therefore, α plays a key role in solar cell design [4].

The intensity of the photon flux decreases exponentially in the semiconductor material. The photon intensity as a function of x for two different values of absorption coefficients is shown in Figure 2.1 [4]. If the absorption coefficient is large, the photons are absorbed over a relatively short distance.

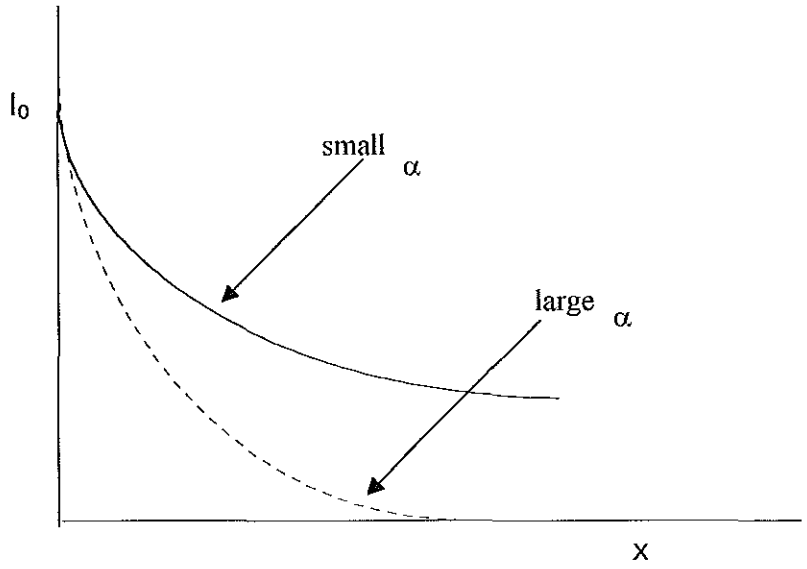

Figure 2.1 *Photon intensity versus distance inside an absorbing material.*

When incident light falls on the surface of the photo-conductor, the increase in conductivity comes from carriers generated either by band-to-band transitions or by transitions involving forbidden-gap energy levels.

Figure 2.2 shows the absorption coefficient for crystalline silicon (c-Si), micro-crystalline silicon (μc-Si:H) and amorphous silicon (a-Si:H) as a function of wavelength.

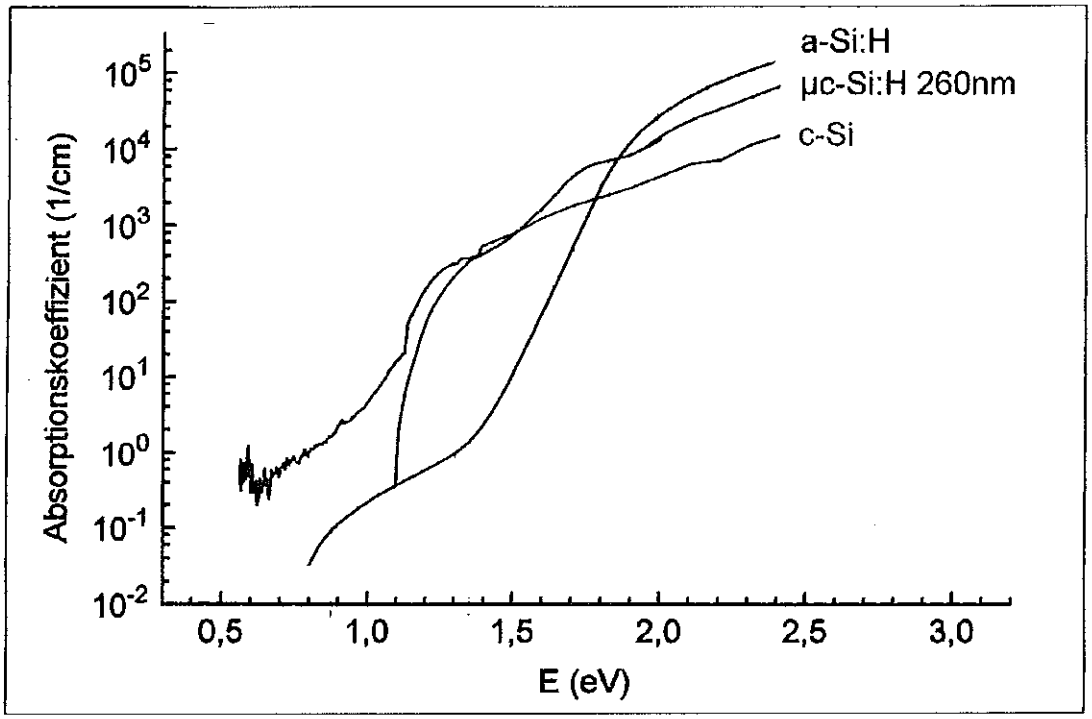

Figure 2.2 *The spectral dependence of the absorption coefficient of crystalline , micro-crystalline and amorphous silicon [6].*

Since α is a strong function of the wavelength for a given semiconductor, the wavelength range in which appreciable photo-current can be generated is limited. The long wavelength cutoff λ_c is established by the energy gap of the semiconductor and is:

$$\lambda_c = \frac{1.24}{E_g(eV)} \ (\mu m) \qquad (2.17)$$

Therefore the long-wavelength cutoff is about 1100 nm for CrSi . For wavelengths longer than λ_c , the values of α are too small to give appreciable absorption. The short-wavelength cutoff of the photo response exists because the values of α for short wavelength are very large ($\sim 10^5$ cm^{-1}), and the radiation is absorbed near the surface where the recombination time is short. The photo-carriers recombine before they are swept out of the area [4].

2.2.2 Current-voltage (I-V) characteristic of solar cells

The I-V characteristics are frequently used to characterize the performance of solar cells.

The total current in the pn junction is the sum of the individual electron and hole currents which are constant through the depletion region. Since the electron and hole currents are continuous functions through the pn junction, the total pn junction current will be the minority carrier hole diffusion current at $x = x_n$ plus the minority electron diffusion current at $x = - x_p$.

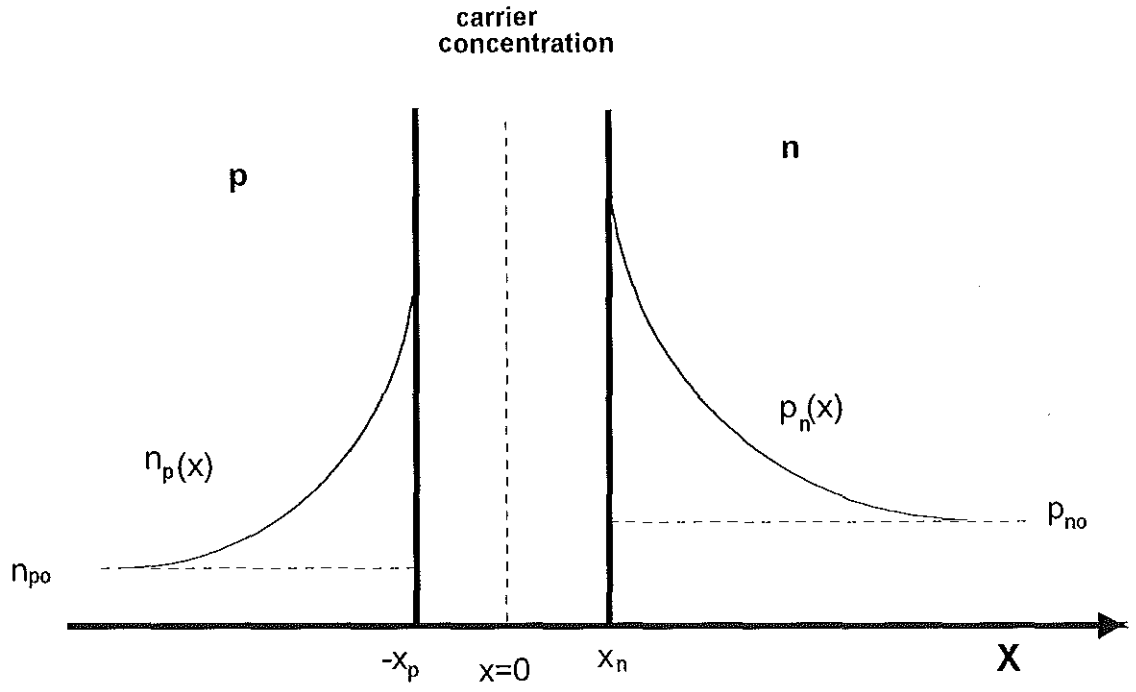

Figure 2.3 *Steady-state minority carrier concentration in a pn-junction under forward bias [4].*

When a forward-bias voltage is applied to the pn junction, the junction is no longer in thermal equilibrium. The forward-bias voltage lowers the potential barrier so that majority carrier electrons from the n-region are injected into the p-region, thereby increasing the minority carrier electron concentration. This produces excess minority carrier electrons in the p-region.

Exactly the same process occurs for majority carrier holes in the p-region which are injected across the space charge region into the n-region under a forward-bias voltage. Figure 2.3 shows these results.

The approach used to determine the current in a pn junction is based on the following three assumptions.

1. The total current is a constant throughout the entire pn structure.
2. The individual electron and hole currents are continuous functions through the pn structure.
3. The individual electron and hole currents are constant throughout the depletion region.

The total current in the junction is the sum of the individual electron and hole currents which are constant through the depletion region. Since the electron and hole currents are continuous functions through the pn junction, the total pn junction current will be the minority carrier hole diffusion current at $x = x_n$ plus the minority carrier electron diffusion current at $x = -x_p$.

The gradients in the minority carrier concentration, as shown in Figure 2.3 , produce diffusion currents, and since we are assuming the electric field to be zero at the space charge edges, we can neglect any minority carrier diffusion current component.

We can calculate the minority carrier hole diffusion current density at $x = x_n$ from the relation [4]:

$$J_p(x_n) = -eD_p \frac{dp_n(x)}{dx}\Big/_{x=x_n} \qquad (2.18)$$

Assuming uniformly doped regions, the thermal equilibrium carrier concentration is constant, so the hole diffusion current density is written as:

$$J_p(x_n) = -eD_p \frac{d(\delta p_n(x))}{dx}\Big/_{x=x_n} \qquad (2.19)$$

The excess carrier concentrations are also found to be:

$$\delta p_n(x) = p_{no}\left[\quad \left(\frac{eV}{kT}\right) - 1\right] \quad \left(\frac{x_n - x}{L_p}\right) \qquad (2.20)$$

Taking the derivative of equation (2. 20) and substituting into equation (2.19), we obtain:

$$J_p(x_n) = \frac{eD_p p_{no}}{L_p}\left[\quad \left(\frac{eV}{kT}\right) - 1\right] \qquad (2.21)$$

Similarly, we may calculate the electron diffusion current density at $x = -x_p$. This may be written as:

$$J_n(-x_p) = eD_n \frac{dn_p(x)}{dx}\Big/_{x=-x_p} \qquad (2.22)$$

and finally we obtain:

$$J_n(-x_p) = \frac{eD_n n_{po}}{L_n}\left[\quad \left(\frac{eV}{kT}\right) - 1\right] \qquad (2.23)$$

The total current density J at the pn junction is then:

$$J = \left[\frac{eD_p p_{no}}{L_p} - \frac{eD_n n_{po}}{L_n}\right]\left[\quad \left(\frac{eV}{kT}\right) - 1\right] \qquad (2.24)$$

We may define a parameter J_s (the saturation current) as:

$$J_S = \left[\frac{eD_p p_{no}}{L_p} - \frac{eD_n n_{po}}{L_n} \right] \qquad (2 . 25)$$

So equation (2.24) may be written as:

$$J = J_S \left[\quad \left(\frac{eV}{kT} \right) - 1 \right] \qquad (2 . 26)$$

Equation (2 . 26), known as the ideal-diode equation, gives a good description of the current-voltage characteristic of the pn junction over a wide range of currents and voltages [4]. The simplest equivalent circuit of the solar cell under radiation is shown in Figure 2.4.

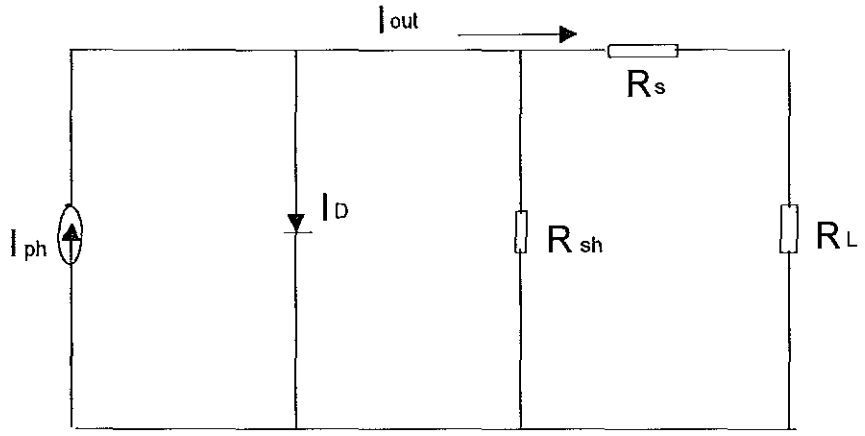

Figure 2.4 *The idealized equivalent circuit of a solar cell .*

The constant current source results from the excitation of excess carriers by radiation. The difference between the diode current (I_D) and the light generated current (I_{ph}) is the output current (I_{out}) which is given by:

$$I_{out} = I_o\left[\quad \left(\frac{eV}{kT}\right) - 1\right] - I_{ph} \qquad (2.27)$$

Where V is the voltage, e the magnitude of the charge, T is the absolute temperature and I_o is the diode saturation current.

The current obtained when V = 0 is called the short-circuit current (I_{sc}) similarly the voltage obtained when I = 0 is called the open-circuit voltage (V_{oc}). An expression for the V_{oc} can be obtained from the equation (2.27), by setting I = 0, as:

$$V_{oc} = \frac{kT}{e}\quad \left(\frac{I_{ph}}{I_o} + 1\right) \qquad (2.28)$$

The power output is equal to the area of the rectangle indicated in figure 2.5. The power output is maximum at the maximum power point [V_m . I_m] , where V_m and I_m are the voltage and the current corresponding to the maximum power point respectively [14].

The energy conversion efficiency (η) of the solar cell is given by :

$$\eta = \frac{V_m I_m}{P_{in}} = \frac{V_{oc} I_{sc}}{P_{in}} FF \qquad (2.29)$$

Where P_{in} is the total power of the light incident on the cell and FF is the fill factor given by:

$$FF = \frac{V_m I_m}{V_{oc} I_{sc}} \qquad (2.30)$$

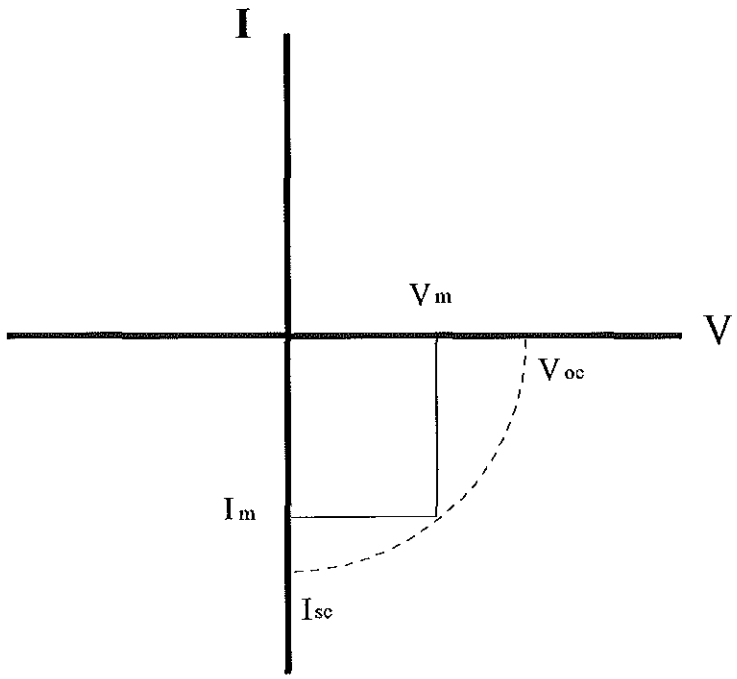

Figure 2.5 *Ideal current voltage characteristic of a solar cell under illumination.*

Grain boundary states play a dominant role in determining the electric and photo-voltaic properties of polycrystalline silicon by acting as traps and recombination centers. The recombination loss at grain boundaries is the predominant loss mechanism in polycrystalline solar cells. Most theoretical calculations have been made for the column grain growth boundary. But all grain boundaries at different physical locations must be taken into account, and the efficiency must be calculated after estimating the

effects of grain boundary states on short-circuit photo-current, open-circuit voltage and fill factor. Cell parameters can be calculated based on a transformation of grain boundary recombination centers to a uniform distribution of such states throughout the grain [1].

3. EXPERIMENTAL APPARATUS

The minority carrier life time (τ) of different silicon solar cells were studied at room temperature (T = 300 K). Open circuit voltage decay (OCVD) technique was used to measure the minority carrier life time. The Nd:YAG (Neodymium doped Yttrium Aluminum Gamete) laser pulses, the nitrogen laser pulses and light pulses from a stroboscope lamp were used to generate excess carriers inside the sample solar cells, causing a momentary increase in conductivity.

The increase in conductivity results in a peak open circuit voltage (V_{oc}). The decay of the V_{oc} was observed with a storage oscilloscope. The minority carrier life time was calculated from the measured decay curves (see Chapter 2.1.).

3.1 The Nd :YAG Laser

Good pumping efficiencies can be obtained from four level laser media. A simplified four level energy diagram of Nd:YAG is shown in (Fig. 3.1).

For this experiment the pumped Nd:YAG laser (MEOS) is used for the generation of short pulses. A pump laser beam produced by a photo diode laser (Fig.3.2.A) controlled by a controller unit LDC: 01 (Fig. 3.2H) is first collimated by a 6 mm focal length lens
(Fig. 3.2B) and focused into a YAG rod (Fig.3.2D) by a 60 mm focal length lens (Fig. 3.2C).

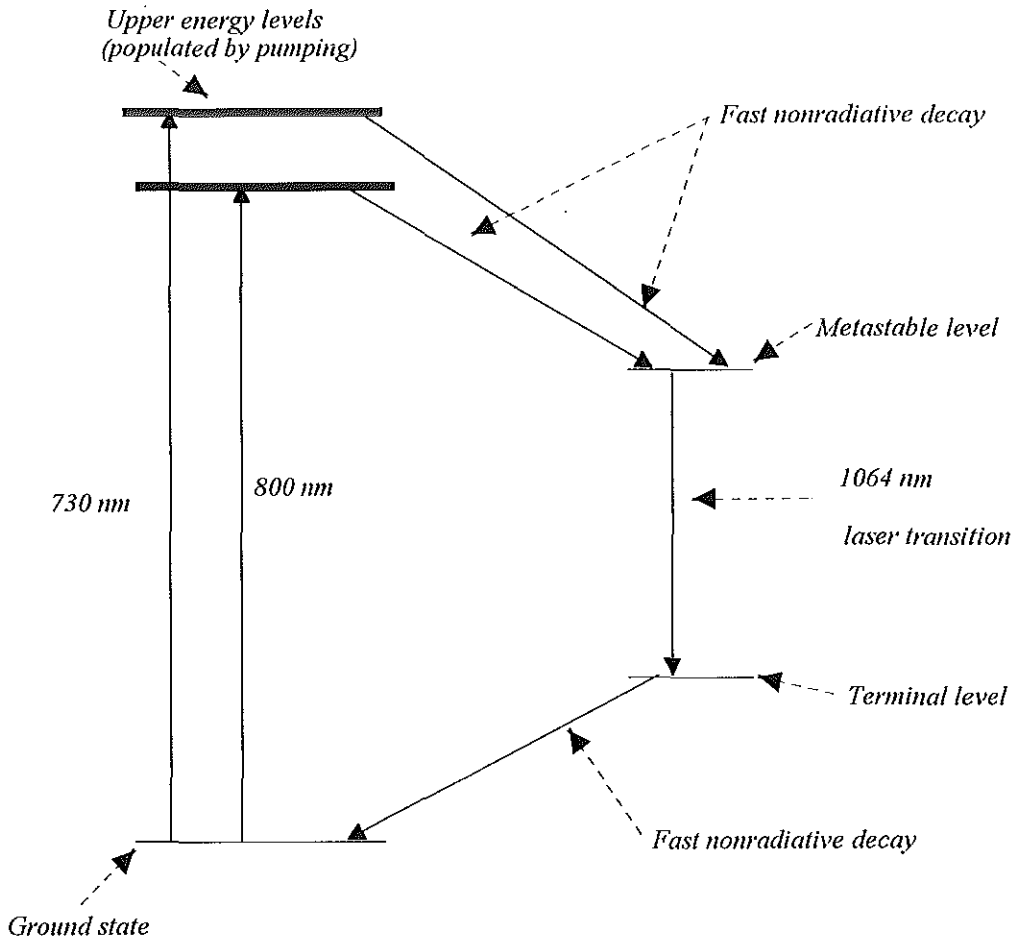

Figure 3.1 *The four level Nd:YAG laser [13].*

The ray traveling along the resonator axis is reflected back and forth between the two laser mirrors (Fig.3.2D & Fig.3.2E). The ray transverses the Neodymium active medium many times resulting in a larger total gain. Then laser radiation at 1064 nm emits on the out put side of the resonator.

The RG1000 filter (Fig.3.2F) is inserted into the path of the beam. The filter absorbs the pump radiation and only the Nd:YAG laser beam is passed through it.

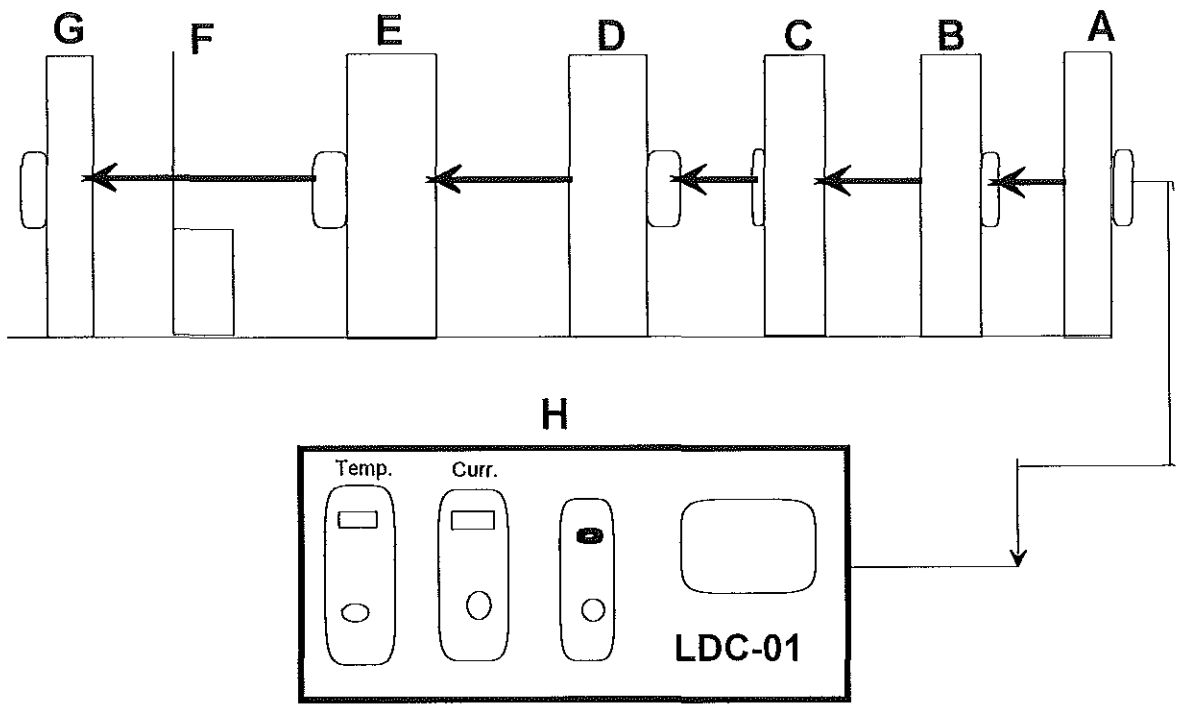

Figure 3.2 *Schematic diagram of the Nd:YAG laser set up*

3.2 Samples

This investigation was conducted with four different silicon solar cells.

1) A monocrystalline silicon solar cell (CrSi-1) produced by Solarex with an effective area of 400 mm^2.

2) A monocrystalline silicon solar cell (CrSi-2) produced by Solarex with an effective area of 1600 mm^2 .

3) A polycrystalline silicon solar cell (poly-CrSi-1) produced by Solaris with an effective area of 2500 mm^2 .

4) A polycrystalline silicon solar cell (poly-CrSi-2) produced by Solaris with an effective area of 10000 mm^2.

For this investigation, the short-circuit current (I_{sc}) and the open-circuit voltage (V_{oc}) of the sample cells were determined experimentally at room temperature and white light illumination of 100 mW/cm^2 as shown in table 3.1.

Name		Manu-facturer	Dimension (mm)	Voc (mV	Isc (mA	Efficie ncy
Crystalline Si	CrSi 1	Solarex	20 x 20	540	114	15.4
	CrSi 2		40 x 40	522	500	16.3
Poly crystalline Si	Poly-CrSi 1	Solaris	50 x 50	480	510	9.8
	Poly-CrSi 2		100 x 100	470	2,100	9.9

Table 3.1 *Solar cell parameters under standard conditions: room temperature and white light illumination of 100 mW/cm^2. V_{oc} is the open-circuit voltage, I_{sc} the short-circuit current.*

3.3 Experimental procedure

The experimental set-up is schematically displayed in Fig.3.3. The Nd:YAG laser beam was split into two parts by a beam splitter. One part was directed to a photo-diode and the other to the sample solar cell.

The sample solar cells were illuminated by Nd:YAG laser pulses of 10^4 Hz and an intensity of 0.02 mW/cm^2. The full width half maximum (FWHM) of these pulses were 6 μsec, which is very short compared to the V_{oc} decay time of the solar cells. The photo-diode (mod.: SFH 202) was the input of the first channel of a 100 MHz digital storage oscilloscope from Hameg (Mod.1007) and used as a reference for the signal from the excitation source.

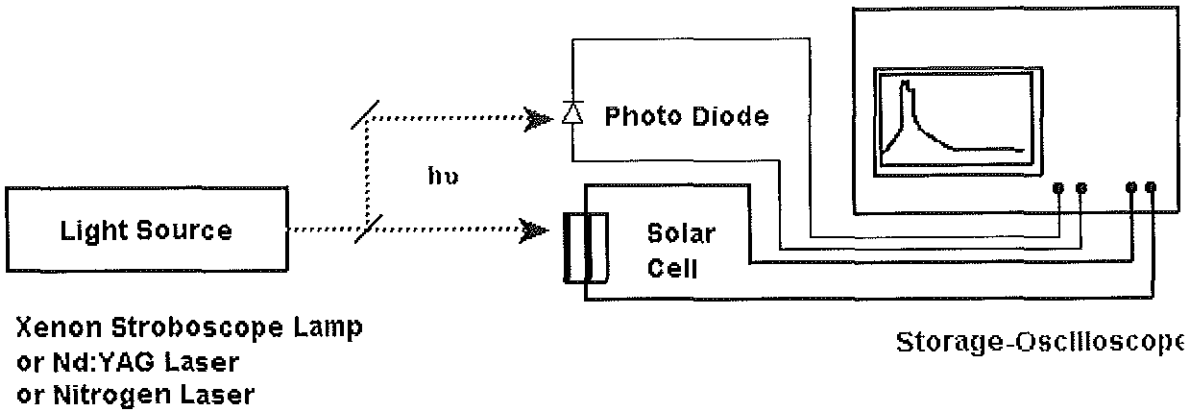

Figure 3.3 *Experimental setup for measuring V_{oc} decay*

The photo-induced open circuit voltage of the sample cells was the input of the second channel of the oscilloscope. The open circuit voltage decay curves change in open circuit voltage (dV_{oc}) and the differential decay time (dt) of the sample solar cells were determined.

In addition to laser excitation, the samples were also illuminated by a light pulse from a xenon stroboscope from Griffin (mod. 65). The experimental otherwise unchanged. The stroboscope has a frequency of 250 Hz, an illumination intensity of 0.58 mW/cm^2, and a FWHM of 22 μsec. The voltage decay (dV_{oc}) and the decay time difference (dt) were determined by OCVD curves.

Finally, the sample photo cells were illuminated by a Nitrogen laser pulse from ORIEL (mod. 79110) . The Nitrogen laser pulses have a frequency of 396 Hz and an illumination intensity of 7.5 mW/cm^2 and a FWHM of 5 nsec.

The parameters of these excitation sources are summarized in table 3.2

LIGHT SOURSE	FWHM (μsec)	Frequency (Hz)	Intensity (mW/cm^2)	Illuminated Area
Xenon Stroboscope Lamp	22	250	0.58	whole sample
Nd:YAG Laser	6	10,000	0.02	0.04 mm^2
Nitrogen Laser	0.005	396	7.5	0.5 cm^2

Table 3.2 *The parameters of the excitation sources.*

The OCVD decay curves and the decay time are observed on an oscilloscope screen. Because of the broadening of the curves and the precision a maximum error of $\pm$ 10% is expected. Then the curves are drawn by hand from the oscilloscope using a transparent paper and scanned to a computer. Four curves for each smaple cells are drawn. Then calculating the standard deviation adds an error of about $\pm$ 10% to the accuracy of the measurements. So totally the accuracy of the minority carrier lifetime determination can be approximated to be within $\pm$ 20% of error.

4. RESULTS AND DISCUSSION

The photo-induced open-circuit voltage decay curves of the pn junction solar cell sample CrSi-1 are shown in Figure 4.1. The change in the open-circuit voltage dV_{oc}, the decay time dt, the calculated minority carrier lifetime τ (equation 2.7), and the calculated diffusion length L (equation 2.15) of each sample cell from the three different excitation sources are shown in table 4.1.

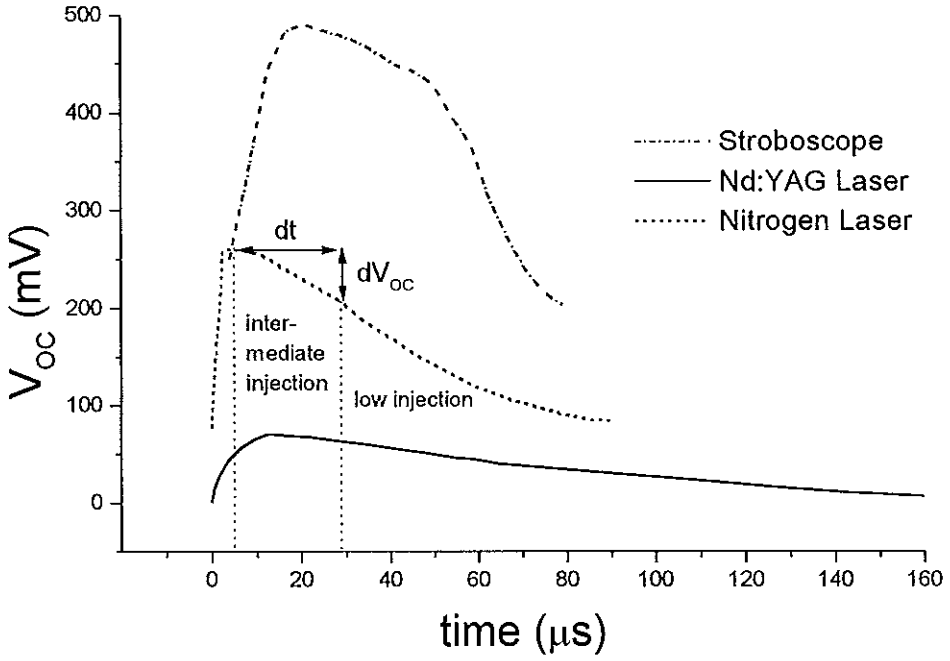

Figure 4.1 *Photo-induced open-circuit voltage decay (OCVD) curves for the crystalline silicon solar cell sample CrSi-1 obtained with a xenon stroboscope lamp, Nd:YAG laser and Nitrogen laser as an excitation source.*

Figure 4.1 shows the photo-induced open-circuit voltage decay curves of one of the investigated pn junction solar cell samples illuminated with a stroboscope lamp (short dots line), with the Nd:YAG laser (bold line) and with the Nitrogen laser (short dash line).

In Figure 4.1 the OCVD spectra demonstrate the existence of two types of decay curve parts. The observed curves initially consist of a nearly linear decay, which gives the decay time dt of the intermediate injection condition. The second part shows an exponentially decaying low injection curve, mainly due to the RC time constant of the solar cells. The high-level injection region is not expected to appear in this case. The excitation sources intensity used for this investigation are not sufficient to produce high injection spectra. The data was taken from the linearly decaying first part of the curves. The curves were copied from the oscilloscope screen using transparent paper and scanned into the computer for further analysis. The results are summarized in table 4.1.

4.1 Crystalline silicon solar cells

The open circuit voltage (V_{OC}) obtained for the solar cell samples excited by the stroboscope lamp is nearly ten times larger than the V_{OC} for the laser excited solar cell. The V_{OC} obtained for the solar cell samples excited by the Nitrogen laser is larger than that of the Nd:YAG laser, but this difference is very small compared to that of the stroboscope lamp. The Nd:YAG laser and the Nitrogen lasers only illuminate a fraction of the solar cell area, 0.04 mm^2 and 0.5 cm^2 respectively, whereas the stroboscope lamp illuminates the whole solar cell area (Table 3.1). This demonstrates that the maximum value of the open-circuit voltage strongly depends on the amount of the solar cell area illuminated by the excitation source.

The minority carrier life time (τ) and the minority carrier diffusion length (L) were obtained to be minimum when the sample solar cells are illuminated by the Nitrogen laser and maximum when illuminated by the Nd:YAG laser (Table 4.1). Thus, the FWHM pulse width

is not related to the minority carrier life time (τ) and minority carrier diffusion length (L) values obtained experimentally.

Solar cell	Exitation source	Max. V_{oc} (mV)	dV_{oc} (mV)	dt µsec)	dVoc/dt (V/sec)	τ (µsec)	L (µm)	µ	L(µm) Reference
CrSi 1	Nd:YAG laser	70	20	30	600	41.7	216.5	450	50 to 1200 [8]
	Strobo scope	400	35	20	1,750	14.3	126.8		
	Nitrogen laser	260	80	36	2,222	11.25	112.5		
CrSi 2	Nd:YAG laser	9.6	12.8	28	457	54.7	244.1		
	Strobo scope	510	120	85	1,411	17.7	141.2		
	Nitrogen laser	200	15	6	2,500	10	106		
Poly - CrSi 1	Nd:YAG laser	6.9	12	9	1,333	18.8	43.3	40	20 to 30[1]
	Strobo scope	590	40	15	2,667	9.4	30.6		
	Nitrogen laser	300	40	9	4,400	5.75	24.9		
Poly - CrSi 2	Nd:YAG laser	6.5	2.6	2.4	1,083	23.1	48		
	Strobo scope	530	50	20	2,500	10	31.6		
	Nitrogen laser	90.5	14	13	1,077	23.25	48.21		

Table 4.1 *Results of the photo-induced open-circuit voltage decay (OCVD) technique measurements with Nd:YAG laser, Nitrogen laser and the stroboscope lamp as an excitation source.*

On the other hand, in Figure 4.2, the spectral dependent emission spectra of the Xenon stroboscope lamp (Left axis, solid line) and the Nd:YAG laser (Left axis, dashed line) are compared with the spectral dependent absorption coefficient for crystalline silicon in the energy range of its absorption edge [6].

The absorption coefficient is displayed on the right axis and drawn as a dashed line. The Nd:YAG laser line at 1.165 eV (1064 nm) is located in a region of low absorption for crystalline silicon. The stroboscope spectrum extends far into the visible spectral range where the crystalline silicon absorbs up to 1000 times stronger than in the near infrared spectral region at the Nd:YAG laser emission. The Nitrogen laser line at 3.678 eV (337.1nm) is in the ultraviolet region where the crystalline silicon absorbs about 100 times stronger than that of the xenon stroboscope lamp in the visible range [4] . Therefore the Nd:YAG laser pulses penetrate deeper into the solar cell than the stroboscope lamp photons and the Nitrogen laser pulses. The Nitrogen laser pulses are absorbed over a relatively short distance compared to the stroboscope lamp and the deeply penetrating Nd:YAG laser pulses (Fig. 2.1).

The CrSi-1 sample has a shorter minority carrier lifetime (τ) and a shorter minority carrier diffusion length (L) than the CrSi-2 sample cell when using Nd:YAG laser pulses and the stroboscope lamp as an excitation sources. Conversely, when the cells are illuminated by the Nitrogen laser pulses the opposite results are observed. All experimentally determined diffusion lengths for both crystalline silicon samples are within the interval of the literature values (Table 4.1).

The absorption coefficient of silicon for the Nitrogen laser emission line at 3.678 eV is about 10^5 cm^{-1} [4]. Using equation (2 .13), it can be calculated that only about 1/e of the initial intensity of the photon flux striking the surface of the cell can travel a distance larger than 0.1 μm deep into the solar cell from its surface.

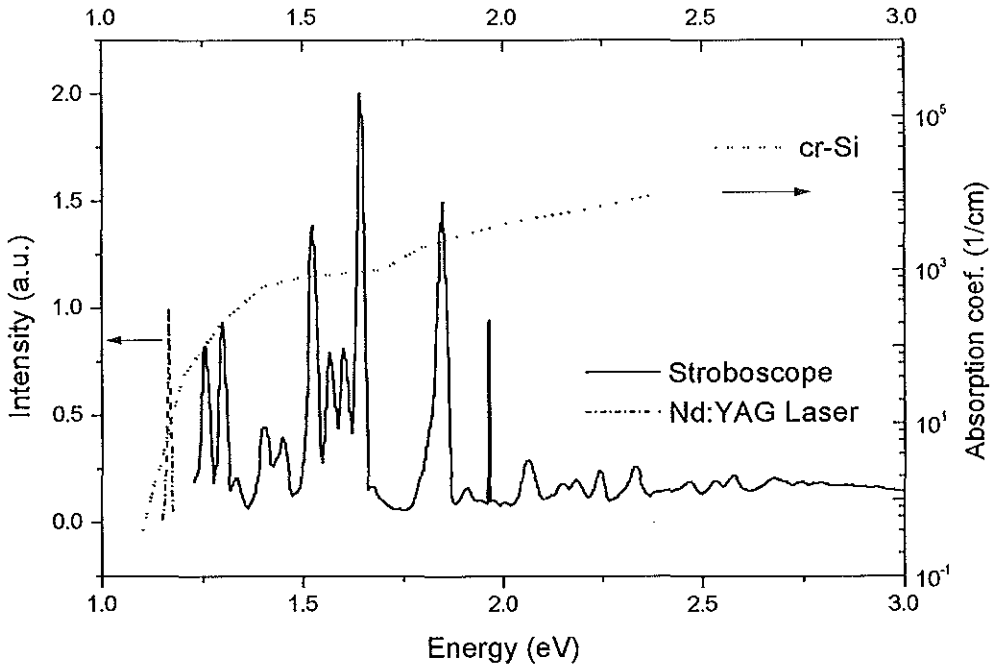

Figure 4.2 *Spectral dependent emission spectra of the xenon stroboscope lamp and the Nd:YAG laser in the energy range of the absorption edge of the crystalline silicon . The energy dependence of the absorption coefficient of crystalline silicon (right axis, dashed line) [6].*

Compared to the thickness of the crystalline silicon (Fig. 1.1), about 99.999917% of the incident photon energy is absorbed within the n-type emitter. The photon energy of the Nitrogen laser entering the p-type base to generate electron-hole pairs is almost negligible compared to the incident photon energy.

Therefore, for crystalline silicon solar cells, the reduced measured minority carrier lifetime and diffusion length measured with the Nitrogen laser compared with the results measured with the Nd:YAG laser is the result of the strong surface absorption of the first excitation source compared to that later one.

4.2 polycrystalline silicon solar cells

The OCVD curves of the polycrystalline silicon solar cell samples have a very similar characteristic to those obtained for the crystalline silicon solar cells (Fig.4.1).

The open-circuit voltage (V_{oc}) determined for the PolyCrSi-1 and PolyCrSi-2 sample solar cells with the stroboscope excitation is about 90 times larger than that with the Nd:YAG laser as an excitation source (Table 4.1). The open-circuit voltage (V_{oc}) for the PolyCrSi-1 and PolyCrSi-2 sample solar cells with Nitrogen laser excitation is, about 50 and 15 times respectively, larger than with that of the Nd:YAG laser. Therefore, comparing these values with the illumination area of the excitation sources (Table 3.1), the maximum open circuit voltage (V_{oc}) of the polycrystalline silicon solar cell is influenced by the amount of the solar cell area illuminated by the excitation sources.

Grain boundary states play a dominant role in determining the electrical and photo-voltaic properties of polycrystalline silicon by acting as traps and recombination centers [9]. The open circuit voltage obtained for PolyCrSi-1 sample cell is larger than that for PolyCrSi-2 with both the stroboscope lamp and the Nd:YAG laser pulses (Table 4.1). But the illuminated area of the PolyCrSi-2 sample solar cell is four times larger than that of the PolyCrSi-1 sample solar cell (Table 3.1). This experimental data suggests that the grain boundary state of the polycrystalline silicon plays a role in determining the electrical properties of polycrystalline silicon.

The minority carrier lifetime (τ) and the minority carrier diffusion length (L) obtained, for both polycrystalline solar cell samples, with a stroboscope lamp is smaller than that obtained with the Nd:YAG laser. But, the difference is very small compared to that observed for the crystalline solar cells. The absorption coefficient of polycrystalline silicon, is

assumed to be similar to that of the crystalline silicon (Fig. 4.2). In the energy range of the strongest stroboscope emission α is larger than in the energy range for the Nd:YAG laser pulse. However, polycrystalline solar cells are about ten times thinner than the crystalline solar cells. So the stroboscope light can penetrate into the p-type base to generate electron-hole pairs. Therefore, the lifetime determined by the Nd:YAG laser excited OCVD spectra is similar to the surface recombination shortened lifetime obtained with the stroboscope excitation.

On the other hand, the minority carrier lifetime and diffusion length obtained for the PolyCrSi-1 sample solar cell with the Nitrogen laser excitation are shorter than those obtained with both the stroboscope and the Nd:YAG laser excitation sources. This is to be expected due to the strong absorption coefficient of polycrystalline silicon for the strongest Nitrogen laser emission. However, the contrary result is observed for the PolyCrSi-2 sample solar cell. This indicates that the minority carrier lifetime and diffusion length of polycrystalline silicon are affected by grain boundary states.

5. CONCLUSION

The minority carrier lifetimes for crystalline silicon solar cells are larger than the polycrystalline solar cells determined in this experiment with the stroboscope lamp and the Nd:YAG laser as an excitation source (Fig. 5.1).

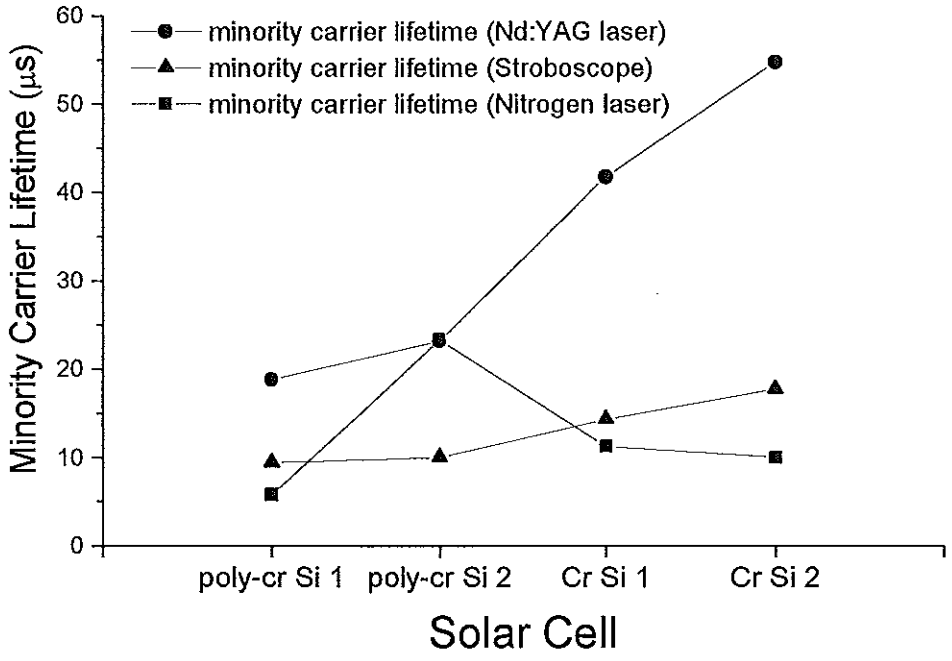

Figure 5.1 *The minority carrier lifetime for the photo-induced open-circuit voltage decay (OCVD) technique measurements of crystalline and polycrystalline silicon solar cells obtained with xenon stroboscope lamp, Nd:YAG laser and Nitrogen laser excitation.*

Since the polycrystalline samples have relatively poor electrical properties compared to the crystalline samples, the minority carrier lifetimes determined in this experiment with the stroboscope lamp and the Nd:YAG laser excitation are reasonable.

There is a strong relation between the different investigated solar cell types and their minority carrier lifetime (τ) and diffusion length (L) (Fig. 5.2).

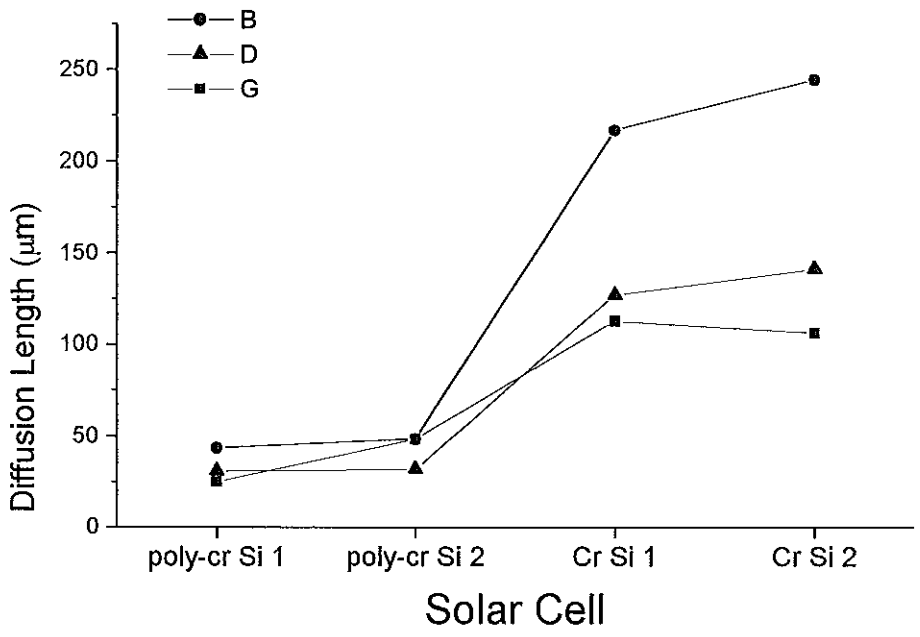

Figure 5.2 *The minority carrier diffusion length for the photo-induced open-circuit voltage decay (OCVD) technique measurements of crystalline and polycrystalline silicon solar cells obtained with xenon stroboscope lamp, Nd:YAG laser and Nitrogen laser.*

The stroboscope excited OCVD measurements of the investigated solar cells produce shorter minority carrier lifetime, compared to the Nd:YAG laser excited measurements, due to the influence of surface absorption. The Nitrogen laser excited OCVD measurements of the solar cells show a complete different trend for the L and τ, compared to the other two excitation sources, due to the very strong

surface absorption. These factors are pronounced in the thicker crystalline solar cell samples.

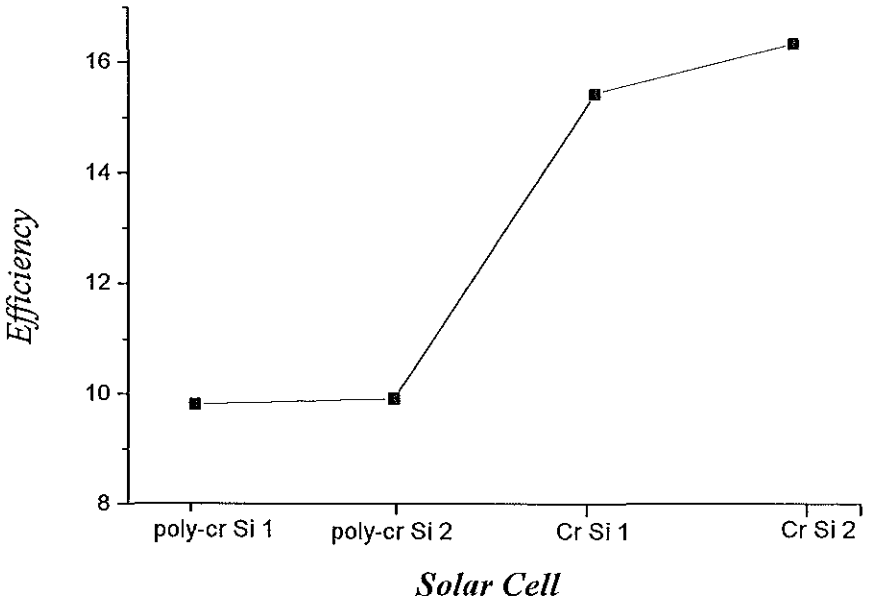

Figure 5.3 *The efficiencies of the sample solar cells in percentage.*

However, the measured minority carrier lifetime (τ) and its correlated diffusion length (L) of the sample cells with the stroboscope lamp and Nd:YAG laser excitations produce good information about the attainable cell efficiency.

The larger the minority carrier lifetime, the larger is the diffusion length and the efficiency of the solar cells (compare fig.5.1, fig 5.2 and fig 5.3).

Therefore, the open-circuit voltage decay (OCVD) technique with the excitation source from either the visible spectral range (xenon stroboscope lamp emission spectrum) or the near infrared spectral region (Nd:YAG laser emission)

is a useful alternative method to the IV characteristics of solar cells to forecast the efficiencies of crystalline and polycrystalline silicon solar cells.

REFERENCES

[1] A.K. Ghosh, C. Fishman and T. Feng, **Theory of the electrical and photo-voltaic properties of polycrystalline silicon,** *J. Appl. Phys.*, **51**(1), 1980, 446-454.

[2] Amensisa Abdi, *Thesis (AAU),* **Optical characterization of thin films for solar cell application,** 1997.

[3] B. H. Rose and H. T. Weaver, **Determination of effective surface recombination velocity and minority carrier lifetime in high-efficiency Si solar cells,** *J. Appl. Phys.*, **54**(1), 1983, 238-247.

[4] D. A. Neamen, **Semiconductor physics and devices,** *Irwin, Boston, 1992*.

[5] Endeshaw Bekele, *Thesis (AAU),* **Optical characterization of thin film solar cells,** 1996.

[6] F. Finger, M. Schmidt and R. Schwarz, **Mikrokristalline Silicium-Schichten fuer Duennschicht-Solarzellen,** *Photovoltaic 3,* Forschungsverbund Sonnenenergie, Themen , 95/96, Koeln, 1995, 81-86.

[7] J. A. Mazer, **Solar cells: An introduction to crystalline photovoltaic technology,** *Kluwer Academic publishers,* Boston, 1997, 102-110.

[8] M. Saritas and H. McKell, **Comparison of minority carrier diffusion length measurements in silicon by the photoconductive decay and surface photovoltaic methods,** *J. Appl. Phys.*, **63**(9), 1988, 4561-4567.

[9] M. R. I. Ramadan, **Effect of minority carrier lifetime in solar cells,** *Solar and wind technology,* **6**, 1989, 615-617.

[10] U. Stutenbaeumer, Belaineh Mesfin and Solomon Beneberu, **Determination of the optical constants and dielectric functions of thin film a-Si:H solar cells. Solar Energy Materials and Solar Cells,** vol.57, 1999, 49-59.

[11] T. J. Coutts and J. D. Meakin, **Current topics in photovoltaics,** Vol.2, 1987, 108-115.

[12] C. Kittel, **Introduction to solid state physics,** *sixth ed., NewYork publisher,* 1986.

[13] T. V. Higgins, **The three phases of lasers:solid state, gas, and liquid laser,** *Focus world,* July 1995, 73-78.

[14] Belaineh Mesfin, *Thesis (AAU),* **A-Si:H multilayer solar cells:optical and electrical properties,** 1998.

[15] U. Stutenbaeumer and Elias Lewetegn, **Comparison of minority carrier diffusion length measurements in silicon solar cells by the photo-induced open-circuit voltage decay (OCVD) with different excitation sources,** *accepted research paper in Renewable Energy, 1999.*